

Numerical investigation towards a HiTAC condition in a 9MW heavy fuel-oil boiler

Shanglong Zhu^{1,*}, Bart Venneker², Dirk Roekaerts³, Artur Pozarlik¹, Theo van der Meer¹

¹ Laboratory of Thermal Engineering, University of Twente, ²Stork Thermeq B.V.,

³ Department of Process and Energy, Delft University of Technology, the Netherlands

Abstract

In this study, several conditions in a 9 MW heavy fuel-oil boiler were numerically studied in order to get a better understanding of the application of HiTAC in such a boiler. Simulations were done with an Euler-Lagrange approach. The Eddy Dissipation model was used for combustion. Simulation results showed that by recycling various ratios of flue gas into the primary and secondary air, a more uniform temperature distribution can be achieved. Besides, thermal NO_x can be reduced to a lower level. Radiation from soot has shown to have a considerable influence on the predicted temperature profiles. It can reduce the peak temperature by 140 K in the case with hot combustion air.

1. Introduction

High temperature air combustion (HiTAC) has been investigated and applied in industry for more than one decade since being introduced [1,2,3,4,5]. In this combustion regime, fuel is oxidized in an environment where combustion air is highly diluted by a substantial amount of inert flue gases. Its temperature is above that of auto-ignition. Thus chemical reactions occur in a distributed zone with a reduced peak temperature [2,6]. As a result, the temperature distribution is more uniform, the net radiation flux can increase by as much as 30% [1], sound generated is lowered and pollutant emissions, NO_x in particular, are much lower than that of conventional combustion. The key features of this high-efficiency combustion process can be utilized to lead to simpler, cheaper and more reliable designs of boilers, with very low emissions of harmful species. Gains could be significant especially for heavy fuel-oils. The HiTAC combustion process lends itself ideally for the combustion of all sorts of “difficult” fuels, ranging from low-calorific gases such as waste-gases, to heavy fuel-oils.

However, to date little is known about spray combustion under HiTAC condition [6], especially about heavy fuel-oil. The IFRF carried out semi-industrial scale tests using both a light and a heavy fuel oil in 1998. Realization of flameless combustion for the light oil was straightforward. It was difficult to visually determine where the combustion takes place since the whole furnace glows without any visible presence of flames. In contrast, the heavy fuel oil flames were luminous and particulate emissions of around 400 mg/Nm³ [7,8]. However, in Seng-Rung Wu’s study [9], reduction of NO_x was observed in heavy fuel-oil combustion. The penetration depths of the jets and the role of buoyancy, employing different locations of fuel oil atomizer in the burner, were found important for the mixing of fuel oil with high temperature air and for the resultant NO_x emission. Several configurations were studied. Two special air-assisted oil atomizers, the effervescent atomizer and

the double mixed-vortex atomizer (DMV) were developed to overcome coking of the heavy fuel oil in the oil atomizer during the regenerator mode. It indicates that the implementation of HiTAC for heavy fuel oil requires more investigations on mixing of reactants and the corresponding chemical mechanisms.

In order to investigate the feasibility of the application of heavy fuel-oil combustion with HiTAC, an industrial 9 MW boiler at Stork Thermeq B.V. will be used in the near future. In the present study, several realizable conditions were numerically studied in order to get a better understanding of the influence of primary and secondary air flow on combustion characteristics and NO_x emissions in this boiler.

2. Experimental setup

The industrial boiler in the present study functions as a test-bed for various burner designs at Stork Thermeq B.V., with air preheating facility and multiple independent combustion air supplies. The furnace room is around 3 m high and around 4.4 m deep. The back of the furnace is partly water-cooled and some evaporator tubes are present at the side walls. The boiler produces up to 12 ton/h of steam at a pressure of 20 bar. A sketch of the boiler is shown in Fig.1.

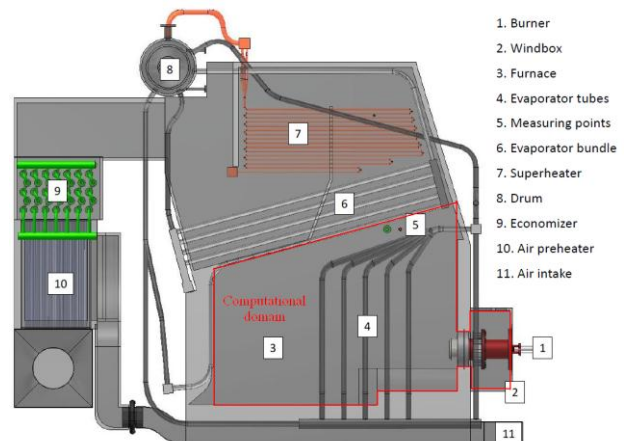


Fig.1. Schematic sketch of the boiler (side view)

* Corresponding author: s.zhu@utwente.nl
Proceedings of the European Combustion Meeting 2013

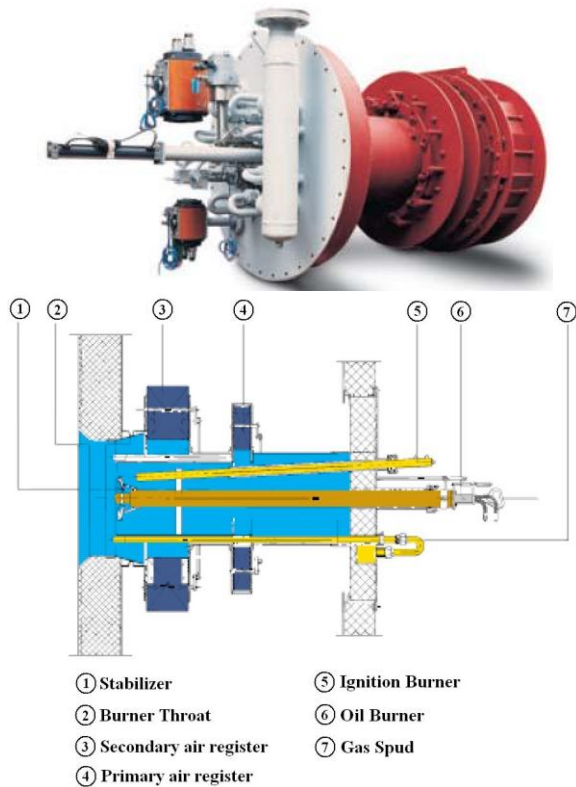


Fig.2. Picture of the DRB burner and a schematic view of the burner

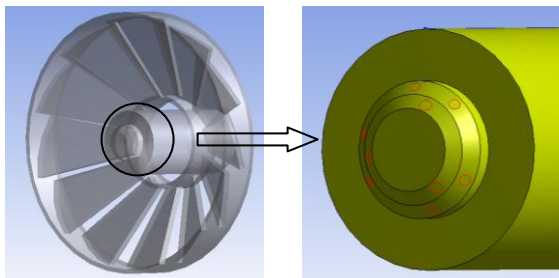


Fig.3. Geometry of the impeller and atomizer in the simulation

The burner used in this boiler is a Stork Double Register Burner (DRB), using an enhanced Y-jet steam assisted atomizer. The steam is injected with the oil in a small channel and this mixture is atomized as it exits the channel. The atomizing steam pressure is 1.5 bar above the oil pressure. Fig.2 shows a picture and the schematic view of the DRB burner. This burner has a proven track record for stable and low- NO_x combustion of a large fuel envelope of liquid as well as gaseous fuels. A typical feature of this burner type is the staged supply of combustion air, using a high amount of rotation. In the sub-stoichiometric primary flame zone, fuel-bound nitrogen is supposed to be converted to N_2 , whereas in the secondary or burnout zone the remainder of the fuel is combusted at a low flame temperature due to the combustion products of the primary zone. The primary air and secondary air go through two separated tunnels in the windbox and

rotate before being injected into the boiler because of the swirl vanes in air registers shown in Fig.2. As shown in Fig.3, the stabilizer consists of 12 impeller blades by which the atomizer with two sets of oil outlets is surrounded. The diameter of the inner outlets is 2.1 mm while the outer is 1.9 mm.

A typical obtained NO_x emission for heavy fuel-oil firing was $550 \text{ mg/m}_0^3 @ 3\% \text{O}_2$ at a firing condition of 4.7 MW and 4vol%, dry O_2 in the flue gases [10].

3. Mathematical models and boundary conditions

3.1. Computational domain, grid and turbulence model

Due to the asymmetric geometry of the boiler and the burner as well as the atomizer, full 3D simulations are carried out. The computational domain consists of the furnace room, the burner and the windbox as shown in Fig.1. Since there is no reaction near the swirl vanes in the air registers or in the windbox, and the presence of them lead to considerable computational cost, the numerical simulation of heavy fuel-oil combustion in this boiler is divided into two steps.

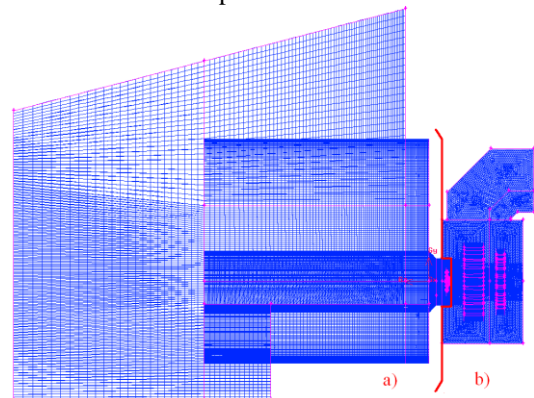


Fig.4. 3D mesh of the computational domain
a) + b): cold state with about 7.5million cells
a): hot state with about 5 million cells

In the first step, the whole computational domain with the air registers and windbox is modelled without a burning spray (cold state), see Fig.4. The calculated velocity components, the kinetic energy k , and the turbulent dissipation ε , at a cross-section between the stabilizer and the air registers are obtained. In the second step, a computational domain downstream this cross-section is employed and the calculated profiles of air flow at this cross-section are used as inlet boundary conditions for the simulation with heavy fuel-oil combustion (hot state). This arrangement allows finer grid in the flame zone, especially in the region close to the atomizer with high speed of steam.

As a result, a 3D mesh with about 7.5 million cells for the cold state and one with about 5 million cells for the hot state are used in the present study (as shown in Fig.4). Based on the comparative analysis of the grid and flow characteristics, the standard $k-\varepsilon$

turbulence model with the standard wall function for the near-wall treatment is employed.

3.2. Spray model

Since the properties of the used heavy fuel-oil, as well as the detailed reaction mechanism are not well known yet, the heavy fuel-oil in the simulation is treated as one single component. Droplets of the fuel are assumed to be fully atomized as spherical droplets of various sizes, with the Rosin- Rammler distribution and a cone angle of 6° according to the empirical data.

The motions of the droplets in the turbulent combustion flow field are calculated using a stochastic tracking method so that the momentum, mass, and energy exchange between the droplets and the gas phase can be simulated by tracking a large number of droplets.

Since the droplets are injected into the boiler by the steam-blast atomizer and are supposed to be well atomized, no secondary break-up or collision process is taken into account in the simulation.

The rate of vaporization is governed by gradient diffusion, with the flux of droplet vapour into the gas phase related to the difference in vapour concentration at the droplet surface and the bulk gas. The concentration of vapour at the droplet surface is evaluated by assuming that the partial pressure of vapour at the interface is equal to the saturated vapour pressure at the droplet temperature.

3.3. Radiation and combustion model

Radiative heat transfer can not be neglected in the simulation of heavy fuel-oil combustion. It contributes to reduce the temperature gradient in the boiler through the presence of CO_2 , H_2O and soot. The Discrete Ordinates (DO) radiation model with a variable absorption coefficient, weighted-sum-of-gray-gases model (WSGGM), is then employed in the simulation.

As combustion model, the Eddy Dissipation Model (ED) is used with a two-step global reaction mechanisms including CO.

3.4. NO_x and soot model

For NO_x formation, there are two major processes contributing to the total NO_x . The first one is known as Thermal NO_x or extended Zeldovich mechanism [11,12], and simply consists of oxidation of atmospheric nitrogen at high temperature conditions. The second one is called Fuel NO_x and describes NO_x creation from nitrogen, which is chemically bounded in liquid fuel. Although prompt NO_x and N_2O intermediate mechanism are also taken into account in the simulation, they showed to have little contribution to the total NO_x formation by a comparative analysis.

Concentration of $[\text{N}]$ is assumed in a quasi-steady state according to its nearly immediate conservation after creation, and concentrations of $[\text{O}]$

and $[\text{OH}]$ are calculated by partial equilibrium approaches [13,14,15].

Fuel NO_x formation is dependent on the local combustion characteristics and the initial concentration of nitrogen-bound compounds. Fuel-bound compounds that contain nitrogen are released into the gas phase when the fuel droplets are heated during the devolatilization stage. Then nitrogen transforms to NO via intermediates, which usually are hydro-cyanide HCN and ammonia NH_3 [16]. In the present study, the intermediate HCN is supposed to be the main route.

For soot formation, the two-step Tesner model [17,18], which predicts the formation of nuclei particles, with soot formation on the nuclei, is employed.

3.5. Boundary conditions

As mentioned above, in the present study, simulation of heavy fuel-oil combustion in the boiler is separated into two steps. In the first step, the inlet boundary conditions of the primary and secondary air are used in the cold state without burning spray. The velocity components, the kinetic energy, k and the turbulent dissipation, ε at a cross-section between the stabilizer and the air registers are then calculated. They are further used in the second step as the inlet boundary conditions of the primary and secondary air at the defined cross-section to simulate the hot state with the burning spray. In a typical case with a power of about 5 MW, a mass flow of 0.5927 kg/s of primary air and a mass flow of 1.7781 kg/s of secondary air is used at a temperature of 373 K.

The lower heating value of the employed heavy fuel-oil is 40.36 MJ/kg and the average molecular weight is about 268 kg/kmol. There is 0.42 wt% nitrogen contained in the fuel-oil. The mass flow of the heavy fuel-oil is 0.1363 kg/s and the steam/oil ratio is about 0.06. The fuel-oil is heated up to 353 K to reach a proper viscosity for atomization and the steam is injected with a temperature of 493 K. Since the properties of the used heavy fuel-oil, as well as the detailed reaction mechanism are not well known yet, the heavy fuel-oil in the simulation is treated as one single component, $\text{C}_{19}\text{H}_{30}$, whose molecular weight is 258 kg/kmol and lower heating value is 40.49 MJ/kg.

An empirical Rosin- Rammler distribution of droplets size with a cone angle of 6° is used in the simulation. The mean diameter of the droplets is $50 \mu\text{m}$. The droplets are assumed to be injected into the boiler through each oil outlet with an initial velocity magnitude of 35 m/s.

Table 1 shows the inlet conditions of air, fuel and steam. The predicted velocity components at the defined cross-section from the first step of cold state lead to mass flow rates of primary and secondary air both within 1% error.

In order to move towards HiTAC conditions, two cases are simulated. In one case (case 1) the

temperature of both primary and secondary air is increased to 746 K, and in the other case (case 2) the mass fraction of O₂ is decreased to half. The above-mentioned two-step simulation is used in both cases.

Tab.1. Inlet conditions of air, fuel and steam

Primary air mass flow rate (kg/s)	0.5927
Secondary air mass flow rate (kg/s)	1.7781
Air temperature (K)	373
O ₂ in the combustion air (wt%)	23.0650
H ₂ O in the combustion air (wt%)	0.7407
Fuel mass flow rate (kg/s)	0.1363
Fuel temperature (K)	353
Steam mass flow rate (kg/s)	0.0082
Steam temperature (K)	493

Tab.2. Inlet conditions of combustion air in four cases

Composition	Case 3		Case 4	
	kg/s	wt%	kg/s	wt%
Primary air				
Percentage of FGR	-	5	-	0
O ₂	0.14268	20.06	0.13671	23.065
CO ₂	0.02046	2.877	0	0
H ₂ O	0.01024	1.44	0.00443	0.747
N ₂	0.53776	75.607	0.45158	76.188
Total	0.71125	100	0.59271	100
Secondary air				
Percentage of FGR	-	15	-	20
O ₂	0.42803	20.06	0.43399	19.269
CO ₂	0.06139	2.877	0.08185	3.634
H ₂ O	0.03072	1.44	0.03653	1.622
N ₂	1.61327	75.607	1.69945	75.454
Total	2.13376	100	2.25231	100
Primary+secondary	2.84502	-	2.84502	-
Composition	Case 5		Case 6	
	kg/s	wt%	kg/s	wt%
Primary air				
Percentage of FGR	-	10	-	8
O ₂	0.14864	17.913	0.14625	18.694
CO ₂	0.04093	4.932	0.03274	4.185
H ₂ O	0.01605	1.934	0.01373	1.755
N ₂	0.62394	75.192	0.58947	75.343
Total	0.8298	100	0.78238	100
Secondary air				
Percentage of FGR	-	10	-	12
O ₂	0.42206	20.944	0.42445	20.578
CO ₂	0.04093	2.031	0.04911	2.381
H ₂ O	0.02491	1.236	0.02723	1.32
N ₂	1.52709	75.778	1.56156	75.707
Ttotal	2.01522	100	2.06264	100
Primary+secondary	2.84502		2.84502	

Furthermore, as will be discussed later, since O₂ concentration shows considerable contribution on the decrease of peak temperature in the boiler, further numerical investigation is done with recycling various ratios of flue gas (FGR) into the primary and secondary air, respectively. It is done for the introduction of various O₂ concentration conditions for the primary and secondary air flow. Four cases which are possible for application in the field test are simulated and compared with the base case. Boundary conditions of the primary and secondary conditions are shown in table 2.

4. Results and Discussion

Fig.5 shows the temperature contours at x=0 mm section of case 1 and case 2 (the same legend) in comparison to the base case. With a preheated combustion air up to 706 K, the peak temperature, T_p in the boiler increases from 2240 K (the base case) to 2390 K. Although the temperature difference between the combustion air temperature and peak temperature T_D , is reduced from 1870 K to 1640 K, the larger peak temperature zone leads to higher NO_x formation in the boiler. Case 2 with reduced O₂ concentration in the combustion air shows a remarkable decrease of T_p , from 2240 K in the base case to 1510 K, and T_D is reduced to 1240 K as shown in table 3. The average NO_x emissions at the outlet of the boiler, M_{NO_x} are also shown in table 3.

Due to 150 K higher of peak temperature, the NO_x emission in case 1 is over two times higher than in the base case, i.e. it increases from 987 mg/m³@3%O₂ to 1992 mg/m³@3%O₂. In contrary, in case 2, NO_x emission is reduced to only 3 mg/m³@3%O₂.

The results of T_p and M_{NO_x} without the soot model are also shown in table 3. The soot model shows considerable influence on the peak temperature and NO_x emission, especially for the case with hot combustion air flow (case 1). The peak temperature is 140 K higher and the NO_x emission is almost three times higher without soot formation in the model. Although the calculated values can only be used qualitatively due to the complexity of the real heavy fuel-oil combustion, the trends demonstrate the influence of temperature and O₂ concentration of combustion air on the flame and NO_x emission. As a result, further investigation is focused on the influence of the O₂ concentration in the primary and secondary air, taking into account the feasibility of operation in the field test (over-reduced O₂ concentration in the combustion air may lead to operating and ignition problems in reality). Various ratios of flue gas are then designed to be recycled and are introduced into the primary and secondary air respectively for introducing various O₂ concentration conditions of combustion air flow.

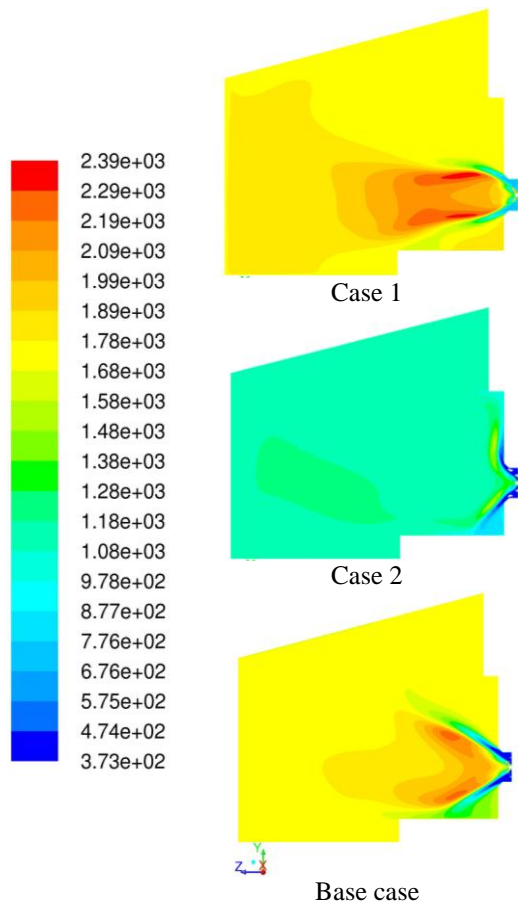


Fig.5 Temperature contours (K) at $x=0$ mm section in case 1, case 2 and the base case

Tab.3. Predicted T_p , T_D and M_{NO_x} in case 1 and case 2 compared with the base case, with and without soot model

	Base case	Case 1	Case 2
Peak temperature T_p (K)	2240	2390	1510
Temperature difference T_D (K)	1870	1640	1240
NO_x emission M_{NO_x} ($mg/m_0^3 @ 3\% O_2$)	987	1192	3
T_p without soot model(K)	2280	2530	1510
M_{NO_x} without soot model ($mg/m_0^3 @ 3\% O_2$)	1470	5337	4

Fig.6 shows the temperature contours at $x=0$ mm section of case 3 to case 6 with the same legend. These cases are compared with the base case. The predicted T_p and T_D , together with M_{NO_x} , is shown in table 4.

According to the investigation on the composition of the NO_x formation in the base case, about 40% percent of the NO_x emission comes from thermal NO_x in the base case. However, with the flue gas recirculation, the structure of the flame changes, especially in case 5 and case 6, whose O_2 concentration in the primary air are reduced more than the other two cases. The peak temperature is

reduced, and in consequence the thermal NO_x emissions are all reduced to a low level in the four cases, leaving the fuel NO_x being the dominant NO_x source. Though in case 5 the NO_x emission is a bit higher than the other cases (in which the fuel NO_x formation is found to be an important effect), its peak temperature is the lowest.

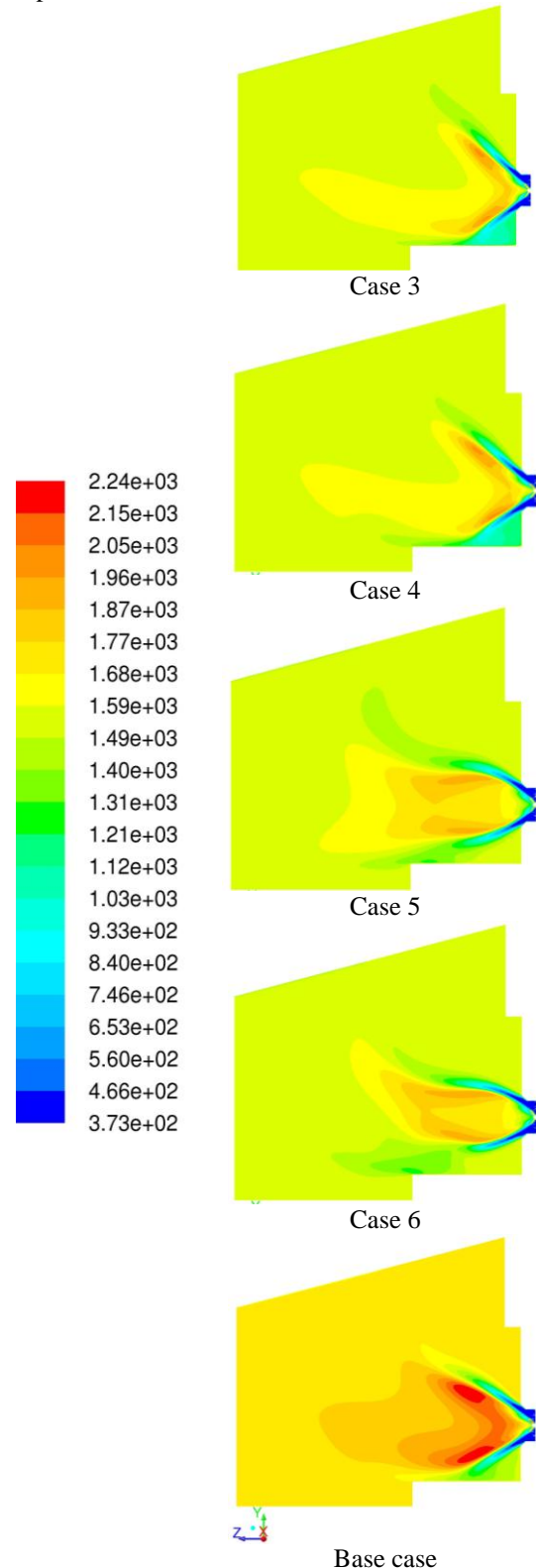


Fig.6 Temperature contours (K) at $x=0$ mm section in case 3 to case 6 compared with the base case

Tab.4. Predicted T_p , T_D and M_{NO_x} in case 3 to case 6

	Case3	Case4	Case5	Case6
Peak temperature T_p (K)	1990	2010	1930	1960
Temperature difference T_D (K)	1620	1640	1560	1590
NO_x emission M_{NO_x} (mg/m ₀ ³ @3%O ₂)	302	292	317	283

5. Conclusions

In the present study, the heavy fuel-oil combustion in a 9MW boiler was numerically investigated. The Euler-Lagrange method and the ED model with a two-step global reaction mechanism were employed. The standard k- ϵ model is used for the turbulence, and an empirical droplet size distribution is used for the spray injected by a steam blast atomizer.

Simulation results with the existing burner showed that increasing of the temperature of the combustion air from 373 K to 746 K leads to a higher peak temperature from 2240 K to 2390 K, while reducing O₂ concentration of the combustion air from 23.065 wt% to 11.5325 wt% results in more uniform temperature distribution with a peak temperature of 1510 K. Further investigation was done with recycling various ratios of flue gas into the primary and secondary air respectively for introducing various O₂ concentration conditions for the combustion air flow. Four cases which are possible for application in the field test were then numerically studied and compared with the base case. The predicted temperature difference between the average temperature and the peak temperature T_D , showed that the case with the lowest O₂ concentration in the primary air has the least temperature difference in the boiler. It was also shown that besides thermal NO_x, fuel NO_x is also one of the dominant contributions to NO_x formation in heavy fuel-oil combustion. By introducing flue gas recirculation, thermal NO_x can be reduced to a very low level, leaving the fuel NO_x playing the dominant role. The interaction between soot and radiation also showed considerable influence on the predicted temperature profiles. In the case with hot combustion air, the peak temperature was reduced by 140 K and the NO_x emission was reduced to about one fourth.

As a result, for heavy fuel-oil combustion, a more uniform temperature distribution in the boiler can be achieved by diluting the primary and secondary air flow with flue gas recirculation and thermal NO_x can be effectively reduced, while the remained fuel NO_x formation is mainly dependent on the local combustion characteristics and the initial concentration of nitrogen-bound compounds. Realization of HiTAC condition in heavy fuel-oil combustion depends on the possibility to guarantee a feasible and sufficiently high level of entrainment of flue gas into the evaporating spray jet.

Acknowledgements

The authors would like to thank the Technology Foundation STW for financial support.

References

- [1] H. Tsuji, A. Gupta, T. Hasegawa, et al., High Temperature Air Combustion: From Energy Conservation to Pollution Reduction, CRC Press, Florida, 2003.
- [2] A. Cavaliere, M. de Joannon, Mild combustion, Prog. Energy Combust. Sci., 30-4 (2004), 329-366.
- [3] L. Blarino, M. Fantuzzi, E. Malfa, U. Zanusso, Tenova Flexytech Burners: Flamesless Combustion for Very Low NO_x Reheating Furnaces, In: Proceedings of the HITAC Conference, Thailand (2007).
- [4] W. Blasiak, W. Yang, Volumetric Combustion of Coal and Biomass in Boilers, In: Proceedings of the HITAC Conference, Thailand (2007).
- [5] Y. Kunio, R&D Commercialization of Innovative Waste-to-energy Technologies, Proceedings of the HITAC Conference, Thailand (2007).
- [6] R. Weber, J. P. Smart, W. vd Kamp, On the (MILD) Combustion of Gaseous, Liquid, and Solid Fuels in High Temperature Preheated Air, Proceedings of the Combustion Institute 30 (2005) 2623-2629.
- [7] A.L. Verlaan, G. Deus Vazquez, M. Kösters, N. Lallemand, S. Orsino, R. Weber, Excess Enthalpy Combustion of Light and Heavy Fuel Oils, Results of High Temperature Air Combustion Trials, IFRF Doc. No. F 46/y/2, 1999.
- [8] R. Weber, S. Orsino, A.L. Verlaan, N. Lallemand, J. Inst. Energy 74 (2001) 38-47.
- [9] S. Wu, W. Chang, J. Chiao, Low NO_x heavy fuel oil combustion with high temperature air. Fuel 86 (2007) 820-828.
- [10] S.J. Dijkstra, B.C.H. Venneker, M.A.F. Derksen, et al., Experiences with Firing Pyrolysis Fuel Oil on Industrial Scale, 25th Deutsche Flammentag, Karlsruhe, Germany (2011).
- [11] J. B. Zeldovich, The Oxidation of Nitrogen in Combustion and Explosion, Acta Physicochimica, 21(1946) 577-628.
- [12] C. T. Bowman, D. J. Seery, Emissions from Continuous Combustion Systems, Plenum Press: New York, 1972.
- [13] J. Warnatz, NO_x Formation in High Temperature Processes, University of Stuttgart, Germany, 2001.
- [14] D. L. Baulch, C. J. Cobos, R. A. Cox, et al., Evaluated Kinetic Data for Combustion Modelling, Journal of Physical and Chemical Reference Data, 21 (1992) 411-734.
- [15] C. K. Westbrook and F. L. Dryer, Chemical Kinetic Modelling of Hydrocarbon Combustion. Progress in Energy and Combustion Science, 10-1 (1984) 1-57.
- [16] T. J. Houser, M. Hull, R. Alway, and T. Biftu, Int. Journal of Chem. Kinet., 12 (1980) 569.
- [17] P. A. Tesner, T. D. Smegiriova, and V. G. Knorre, Kinetics of Dispersed Carbon. Formation, Combustion and Flame, 17-2 (1971) 253-260.
- [18] B.F. Magnussen, B.H. Hjertager, On Mathematical Modelling of Turbulent Combustion with Special Emphasis on Soot Formation and Combustion, 16th Symp. (Int.) on Combustion, 16-1 (1977) 719-729.